JCPT

Modelling of Convective Mixing in CO_2 Storage

H. HASSANZADEH, M. POOLADI-DARVISH, D.W. KEITH
University of Calgary

Abstract

Accurate modelling of the fate of injected CO_2 is necessary if geological storage is to be used at a large scale. In one form of geological storage, CO_2 is injected into an aquifer that has a sealing caprock, forming a CO_2 cap beneath the caprock. The diffusion of CO_2 into underlying formation waters increases the density of water near the top of the aquifer, bringing the system to a hydro-dynamically unstable state. Instabilities can arise from the combination of an unstable density profile and inherent perturbations within the system, e.g., formation heterogeneity. If created, this instability causes convective mixing and greatly accelerates the dissolution of CO_2 into the aquifer. Accurate estimation of the rate of dissolution is important for risk assessments because the timescale for dissolution is the timescale over which the CO_2 has a chance to leak through the caprock or any imperfectly sealed wells.

A new 2D numerical model which has been developed to study the diffusive and convective mixing in geological storage of CO_2 is described. Effects of different formation parameters are investigated in this paper. Results reveal that there are two different timescales involved. The first timescale is the time to onset the instability and the second one is the time to achieve ultimate dissolution. Depending on system Rayleigh number and the formation heterogeneity, convective mixing can greatly accelerate the dissolution of CO_2 in an aquifer. Two field scale problems were studied. In the first, based on the Nisku aquifer, more than 60% of the ultimate dissolution was achieved after 800 years, while the computed timescale for dissolution in the same aquifer in the absence of convection was orders of magnitude larger. In the case of the Glauconitic sandstone aquifer, there was no convective instability. Results suggest that the presence and strength of convective instability should play an important role in choosing aquifers for CO_2 storage.

Introduction

The use of technologies to capture and store CO_2 is rapidly emerging as a potentially important tool for managing carbon emissions. Geological storage, defined as the process of injecting CO_2 into geologic formations for the explicit purpose of avoiding atmospheric emission of CO_2, is perhaps the most important near-term option. Geological storage promises to reduce the cost of achieving deep reductions in CO_2 emissions over the next few decades. While the technologies required to inject CO_2 deep underground are well established in the upstream oil and gas sector, with such methods as CO_2-EOR[1,2] and Acid Gas disposal[3], methods for assessing and monitoring the long-term fate of CO_2, and for assessing the risk of leakage, are in their infancy. Assessments of the risk of leakage of CO_2 from a storage formation may need to analyze leakage mechanisms and their likelihood of occurrence during the full-time period over which mobile free-phase CO_2 is expected to remain in the reservoir. Once dissolved, risk assessments may well ignore the leakage pathways resulting from the very slow movement of CO_2-saturated brines. An accurate assessment of the timescales for dissolution are therefore of the first order of importance.

The CO_2 injected into a saline reservoir is typically 40 – 60% less dense than the resident brines[4]. Driven by density contrasts, CO_2 will flow horizontally (in a horizontal aquifer) spreading under the caprock, and flow upwards, potentially leaking through any high permeability zones or artificial penetrations, such as abandoned wells. The free-phase CO_2 (usually supercritical fluid) slowly dissolves in the brines. The resulting CO_2-rich brines are slightly denser than undersaturated brines, making them negatively buoyant, and thus greatly reducing or eliminating the possibility of leakage. The rate of dissolution depends on the rate at which diffusion or convection brings undersaturated brine in contact with CO_2. Convective mixing enhances the dissolution rate as compared to diffusion by distributing the CO_2 into the aquifer[5]. Therefore, the role of convective mixing in CO_2 sequestration and the timescales involved in the process are important. The dissolution time of the injected CO_2 into brine is important because during this time the injected CO_2 has a chance to leak into the atmosphere through the caprock and wellbores.

Accurate modelling of the convective mixing in heterogeneous porous media plays a central role in predicting the fate of CO_2 injected into aquifers. In this paper, geological CO_2 storage is modelled by solving the convection-diffusion equation while considering the CO_2-brine interface as a boundary condition. Geochemical reactions that can reduce the timescale of sequestration of CO_2 are not included, since they generally occur on longer timescales[6].

The paper is organized as follows. First, the mathematical model for simulating density-driven flow through porous media is briefly presented. The model is validated with a benchmark problem for density-driven flow in porous media. Then, the geological CO_2 sequestrations both in small and field scale are simulated using the model. Two important timescales, the effect of formation properties, as well as sensitivity to temporal and spatial discretisations, are discussed. Finally, the results are summarized and their relevance to geological storage of CO_2 in aquifers is discussed.

Mathematical Model

The governing equations of density-driven flow in saturated porous media are derived from mass and momentum conservation laws. Considering two-dimensional, gravitationally driven fluid

PEER REVIEWED PAPER ("REVIEW AND PUBLICATION PROCESS" CAN BE FOUND ON OUR WEB SITE)

flow, the resulting equations from conservation laws will be fluid flow and mass transport equations. The fluid flow equation is presented in terms of pressure. The mass transport equation is presented in terms of solute or invading component concentration. The governing equations are a set of non-linear partial differential equations coupled through the dependence of viscosity and density on solute concentration, as given by Equations (1) – (3)[7]:

$$\nabla \cdot v^c = 0 \quad \text{..... (1)}$$

$$v^c = -\frac{k}{\mu}\left[\nabla p - \rho g \nabla z\right] \quad \text{..... (2)}$$

$$\phi \frac{\partial C}{\partial t} = \nabla \cdot \left[D \nabla C - C v^c\right] \quad \text{..... (3)}$$

where z is vertical distance and positive downwards, v^c is the single-phase Darcy velocity, k is the permeability, C is the concentration of the invading component (e.g., CO_2), ρ is the mixture density, μ is the mixture viscosity, D is the effective molecular diffusion coefficient, p is pressure, g is gravity constant, t is time, and ϕ is porosity. Permeability and porosity can be arbitrary functions of space. Both mixture density and viscosity are functions of concentration. By considering the CO_2 cap as a boundary condition, the flow is assumed to be single-phase. In addition, it is assumed that the brine is incompressible and Boussinesq fluid approximation is valid[8].

Numerical Implementation

The model is discretised as follows: the pressure equation is discretised implicitly using the finite difference method. An implicit scheme is used for the dispersive part of the transport equation while the convective part is solved explicitly. These types of discretisation have been reported in the literature for solving density-driven flow in porous media[9-15]. A second version of the model was developed to solve both convective and dispersive parts of the transport equation explicitly.

The grid system used in the numerical discretisation of flow and transport equations is a block-centred Cartesian grid. Grid blocks can be uniform or non-uniform. Numerical discretisation of the pressure and transport equations leads to a system of non-linear equations that can be solved to find the spatial and temporal distribution of velocity, pressure, and concentration. These two systems of equations take the form of a penta-diagonal matrix. The Picard iteration method was used to solve the system of non-linear equations[16].

The Courant number, C_R, and the grid Peclet number, Pe, control the oscillations due to the time and spatial discretisations, respectively[17]. The Courant number represents the fraction of a grid block, in which species convect in a single time step and it should be less than one to obtain an accurate solution. The Peclet number represents the importance of convective to diffusive mass fluxes.

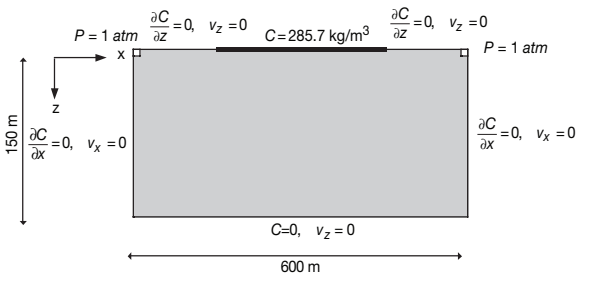

FIGURE 1: Model geometry and boundary conditions for the Elder problem[23].

Numerical solutions are typically oscillation-free with a small numerical error when the following criteria are met:

$$C_{Ri} = \frac{v_i^c \Delta t}{\Delta l_i} \le 1$$

$$Pe_i = \frac{v_i^c \Delta l_i}{D_i} \le 2 \quad \text{..... (4)}$$

where C_{Ri} and Pe_i are grid Courant and Peclet numbers, respectively. In addition to these constraints, it has been suggested that for multi-dimensional problems, the following condition should be satisfied[18,19].

$$C_{Ri} = \frac{v_i^c \Delta t}{\Delta l_i} \le \frac{Pe_i}{2} \quad \text{..... (5)}$$

where subscript i refers to the grid block index, Δl is the grid block size, and v is the pore fluid velocity. The time step is calculated based on an automatic selection criterion given by Eliassi and Glass[20].

Equations (1) – (3) are the governing differential equations for density-driven flow in porous media. In order to solve the problem, suitable initial and boundary conditions must accompany the coupled equations. Since different boundary conditions are used, the appropriate initial and boundary conditions are presented independently in different sections. In the next section, the model is validated against a well-known benchmark problem.

Validation With the Elder Benchmark Problem

Elder studied the laminar fluid flow in a box shaped vertical model[21,22]. The flow of fluid in the model was initiated by a vertical temperature gradient. The density gradient generated by the temperature variation caused a complex flow pattern of fingers and lobes. Elder studied the problem both experimentally and numerically. Voss and Souza[23] recast the Elder problem as a variable-density ground-water problem where the fluid density is a function of salt concentration. The Elder problem has been studied extensively in the ground-water literature[10,11,13,15,23,24].

The geometry and boundary conditions of the Elder problem are shown in Figure 1. The upper left and right of the domain are maintained at constant head values of atmospheric pressure and the domain is closed to flow all around. The bottom boundary is at zero salt concentration and the lateral boundaries are closed with respect to concentration. A constant concentration boundary is specified at the middle half of the top boundary. Other parameters related to the problem are given in Table 1[23]. The 600 × 150 m domain initially has zero salt concentration. The maximum fluid density for the Elder salt convection problem is 1,200 kg/m^3. Salt diffuses by molecular diffusion into the domain. The diffused salt makes water at the top denser than water at the bottom layers and eventually creates convective mixing. These flow patterns enhance the mixing process by distributing the salt in the aquifer.

The finite element grid block used as reference solution consists of 3,131 nodes (101 horizontal and 31 vertical) and 6,000 right-angled triangular elements[24]. In this study, 88 by 54 grid blocks were used in x and z directions, respectively. Initial concentration within the model was set to zero. A linear relationship for density as a function of concentration was used, $\rho = \rho_0(1 + \beta_\rho C)$ where β_ρ = 0.0007 m^3/kg corresponds to a maximum density of 1,200 kg/m^3

TABLE 1: Simulation parameters for the Elder problem[23].

Parameter	Symbol	Values
Porosity	ϕ	0.10
Permeability, m^2	k	4.845×10^{-13}
Molecular diffusivity, m^2/sec	D	3.565×10^{-6}

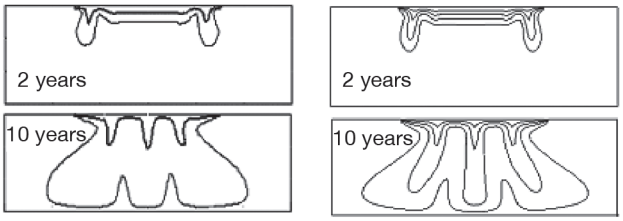

FIGURE 2: Evolution of the flow pattern of the dense fluid into the aquifer for the Elder problem. In this figure, the plots on the left give 0.2 and 0.6 concentration contours from Reference (24), and the results of this study are presented on the right, showing contours for 0.2, 0.4, 0.6, and 0.8 concentrations.

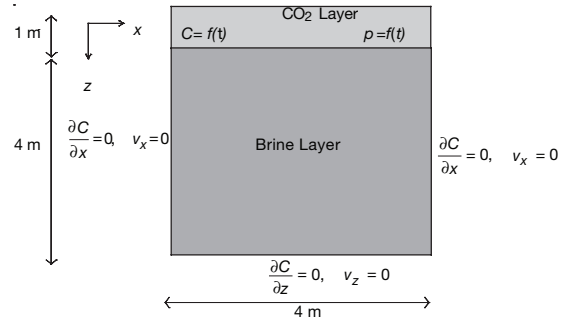

FIGURE 3: Geometry and boundary conditions for the mechanistic study.

for salt water. The viscosity was considered to be constant, similar to the original Elder problem. Salt concentrations for 2 and 10 years are compared with one of the solutions reported in the literature in Figure 2[24]. The comparison shows a reasonable match between the salinity patterns from this study and the reference solution. It is noted that, there are many solutions for the Elder problem in literature that differ slightly depending on the numerical discretisation schemes and approximation used[10,11,13,15,23,24].

In the next section, the governing mechanisms of dissolution of CO_2 in aquifers are described. Then, the developed model is used to investigate the instabilities and how the resulting convective mixing enhances the rate of dissolution.

Mechanistic Studies

A system is stable with respect to a given perturbation if the system relaxes to the initial state when perturbed. It is unstable if the initial perturbation grows with time so that the system departs from its initial state and does not return to it[8]. In geological storage, CO_2 is injected into an aquifer that has a sealing rock, beneath which forms a CO_2 cap. The injected CO_2 starts to diffuse into the formation water. Dissolution of CO_2 increases the brine density up to 2 – 3% in the temperature range of 5 – 300° C[25,26]. The formation water in contact with the CO_2 cap becomes saturated with CO_2 and gains a higher density than the underlying formation water. Therefore, the diffusion of the injected CO_2 into the brine brings the system to a hydro-dynamically unstable state. This unstable state can lead to convective mixing that improves the dissolution by continuously removing CO_2-saturated water from the region adjacent to the CO_2 plume and bringing in undersaturated water[5]. Correct estimation of rate of dissolution is important because the timescale for dissolution is the timescale over which CO_2 has a chance to leak through the caprock.

The fluid in aquifer is in the liquid state and the CO_2 is dissolved into the brine at the interface. In order to avoid the complications arising from a full treatment of two-phase flow, the CO_2-brine interface layer is simulated by imposing a concentration boundary condition appropriate for partial pressure of the overlying CO_2[27, 28]. The fluid in aquifer is assumed to have zero initial CO_2 concentration. The problem geometry and boundary conditions are shown in Figure 3. Other parameters related to the problem are given in Table 2. The maximum density increase due to CO_2 dissolution was assumed to be 1%. The pertinent data were adopted from Ennis-King and Paterson[27, 28]. In all simulations, a linear relationship for density as a function of concentration is considered as given by $\rho = \rho_0(1 + \beta_\rho C)$, where β_ρ is a function of CO_2 solubility in the formation water and changes with time, while the viscosity is considered to be constant. Chang et al.'s correlation, which is based on the experimental data of Wiebe and Gaddy, is used to calculate the CO_2 solubility in water[29, 30]. The CO_2 density is calculated based on Hall and Yarborough's equation of state[31].

TABLE 2: Simulation parameters for the CO_2 mechanistic studies[27].

Parameter	Symbol	Values
Porosity	ϕ	0.20
Horizontal permeability, m^2	k_x	4.845×10^{-13}
Vertical permeability, m^2	k_y	4.845×10^{-14}
Molecular diffusivity, m^2/sec	D	1×10^{-9}
Temperature, ° C	T	78
Initial pressure, MPa	p	18
Gas layer thickness, m	h	1.0
Mixture viscosity, Pa•s	μ	0.0005

In order to accurately simulate convective mixing, a small part of an aquifer was selected for the base-case study. The small-scale study helps to develop a better understanding of the finger growth mechanism. The model has 4 m width and 4 m depth. The thickness of the CO_2 layer at the top of the brine is 1 m. Initial concentration within the model was set to zero. The simulation was started with a small time step and increased based on the automatic selection criterion. The dissolution of CO_2 into the brine results in a pressure reduction in the CO_2 layer. Therefore, the CO_2 concentration at the interface, which corresponds to the equilibrium concentration at that pressure, changes with time, leading to a time-dependent boundary condition.

Bachu and Adams defined the ultimate dissolution as the total amount of CO_2 that can dissolve to saturation in the formation water of the aquifer as[32]:

$$c = V_p \left(C^* - C_i \right) \quad \text{.....(6)}$$

where C_i and C^* are the CO_2 initial and equilibrium concentration at the initial pressure, respectively, and V_p is the aquifer pore volume. The total amount of carbon dioxide dissolved at any time divided by the ultimate CO_2 dissolution is the fraction of ultimate dissolution. In the following, the results are presented in terms of the fraction of ultimate dissolution vs. time, as a measure of the effectiveness of the dissolution process.

Numerical and Physical Disturbances

Generation of density-driven convective mixing patterns requires two criteria: 1) availability of an unstable density field due to the presence of a higher density fluid above a lower density one; and, 2) some disturbance that, in the presence of the unstable field, would grow to macroscopic fingers. In theoretical stability analysis, the growth of infinitesimally small perturbations is studied. These studies have indicated that the small instabilities grow, provided that a minimum instability criterion, characterized by a minimum Rayleigh number, is met[33-35].

$$Ra = \frac{kg\Delta\rho H}{D\phi\mu} \quad \text{.....(7)}$$

In real porous medium, there are many factors that could seed perturbations such as variations in tortuosity, porosity, permeability, and so on. In the following, the role of physical perturbations was examined by imposing variations in the permeability field,

TABLE 3: Details of the simulation data and parameters used for the mechanistic study. In all cases, the domain was discretised to a 60 × 60 grid block system.

Permeability Variations	Permeability Variations	Max. Time Step Days	Max. Peclet Number	Max. Courant Number	Numerical Scheme
Case 1	Homogenous	11.8	1.67	0.38	Implicit
Case 2	0.1 % (random)	1.2	1.67	0.04	Explicit
Case 3	0.1 % (random)	5.8	1.67	0.19	Implicit
Case 4	0.1 % (random)	11.8	1.67	0.38	Implicit
Case 5	0.5 % (random)	11.8	1.67	0.38	Implicit
Case 6*	Homogenous	11.8	1.67	0.38	Implicit

* Case 6 is a hypothetical pure diffusion case.

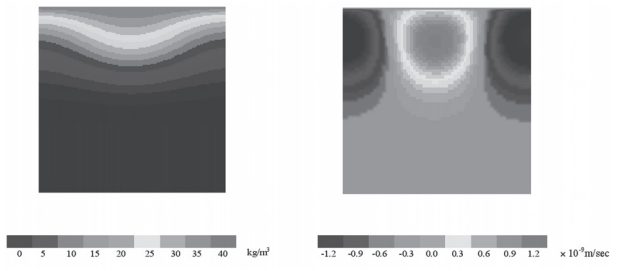

FIGURE 4: Concentration profile (left) in kg/m^3 and vertical velocity profile (right) in m/sec after 31 years. The velocity profile shows generation of convection cells. The maximum vertical velocity is 1.2 × 10^{-9}m/sec.

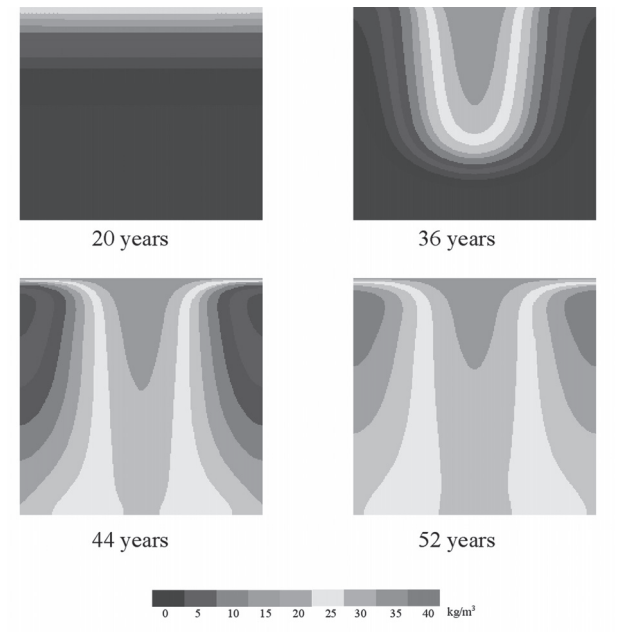

FIGURE 5: Evolution of CO_2 finger for Case 1 at different times. Plates show the concentration distribution of the dissolved CO_2 at different time for a homogenous porous medium case.

and numerical disturbances by varying the discretisation schemes. Table 3 gives the list of cases studied and their details.

In Case 1, the domain was discretised to 60 × 60 grid block system to demonstrate the rate of dissolution for a homogeneous aquifer. As noted previously, for convective mixing to occur some sort of perturbations is required. In numerical models when the porous medium is assumed homogenous, the numerical artifacts could act as a disturbance initiating the instabilities. Depending on the temporal and spatial discretisation and the convergence criteria, each numerical scheme has a different error component that consists of different wavelengths. These kinds of numerical disturbances are difficult to control and grid convergence is difficult to achieve. Figure 4 shows concentration profile and convection

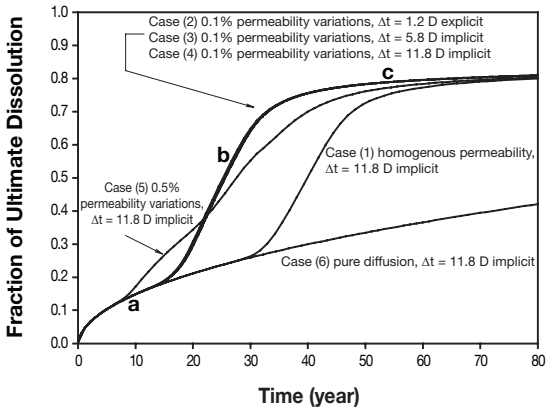

FIGURE 6: Fraction of ultimate dissolution for different cases given in Table 3. In all cases, the domain is discretised into 60 × 60 grid blocks. Results for 0.1% variations in permeability (Cases 2, 3, and 4) using different time steps (t = 1.2, 5.8, and 11.8 D) are the same.

cells that are generated after 31 years for Case 1. Figure 5 shows the evolution of CO_2 fingers in the domain at different times for the same case. For this model geometry, the size of the convection cells is almost 2 m and only one finger of dense saturated brine penetrates the less dense brine.

To examine the role of numerical errors in formation of instabilities in the homogeneous aquifer of Case 1, the time for the onset of instability was compared with the theoretically derived value, which is based on an infinitesimal perturbation. The onset of instability based on free convection in a porous layer of infinite horizontal extent is given by Tan et al.[36-38] as:

$$t_c = 2,262\left[\frac{\mu\phi\sqrt{D}}{kg\Delta\rho}\right]^2 \quad \text{..... (8)}$$

Tan et al.[36-38] used a transient concentration profile and the classical critical Rayleigh number of $4\pi^2$ to drive the above equation. It is noted that the classical critical Rayleigh number of $4\pi^2$ has been derived for a laterally infinite porous medium layer with an initial steady-state temperature distribution and boundary conditions of constant top and bottom temperature[35]. In Figure 6, the dissolution rate for Case 1 increases at about 32 years, which is close to the theoretical value of 32.8 years for the onset of instability calculated by Equation (8), suggesting that the numerical errors are close to the infinitesimal theoretical values. Numerical experiments were performed to investigate the sensitivity of onset of convection to grid-block size for cases when the instabilities were driven numerically. Results (not shown here) reveal that for cases with grid Peclet number, less than two solutions are not sensitive to the spatial discretisations. This Peclet number condition is honoured in all computations presented here.

Real geological formation permeability variations may be controlled by depositional and erosional processes (e.g., high-permeability channel deposits) or structural features (e.g., fractures) and are not totally random. However, random permeability variations of low amplitude were used to seed the perturbation. Next, a

TABLE 4: Aquifer properties used in case studies of Alberta basin aquifers [40].

Aquifer	Thickness (m)	Permeability (m^2)	Gas Cap Pressure After Injection Phase (MPa)	Porosity (%)	Temperature (° C)	Salinity (g/L)	Diffusivity Coefficient (m^2/sec)
Nisku	60	47×10^{-15}	38	9	60	190	4.294×10^{-9}
Glauconitic Ss	13	6×10^{-15}	30	9	50	40	3.553×10^{-9}

permeability field with 0.1% random variation was generated[39]. In Cases 2, 3, and 4, simulations were performed with the same spatial discretisation as in Case 1 but with different time steps and numerical schemes to ensure that the instabilities were controlled by variations in the permeability field, and not by numerical perturbations. Figure 6 shows the fraction of ultimate dissolution by the aquifer vs. time, and demonstrates three mixing periods. The first period is Part A, where the dominant process is diffusion, and the rate of dissolution is slow and depends on the molecular diffusion coefficient. The duration of this period depends on the fluid and rock properties. Part B starts with the generation of growing instabilities at the interface and is related to the Rayleigh number of the problem and the magnitude of the heterogeneities. The rate of dissolution in this period is much higher than the pure diffusion process and most of the dissolution happens during this period. Convective mixing distributes the dissolved CO_2 into the formation and stratifies the density gradients. Stratification of the density gradients diminishes the convection velocity and leads to a lower rate of dissolution in Part C. During this period, the density gradients diminish and the convection cells gradually die down.

The results for Cases 2, 3, and 4, shown in Figure 6, have the same permeability variation of 0.1%, but different temporal discretisation schemes. These results demonstrate that the mixing behaviour for these cases does not depend on the numerical scheme but is governed by the magnitude of the permeability variation. The effect of permeability variation is investigated in Case 5. Figure 6 demonstrates that for Case 5, with 0.5% random permeability variations, the time to start the convective mixing is much smaller than other cases.

Case 6 in Figure 6 demonstrates a hypothetical case, in the absence of convective mixing where dissolution is due to diffusion only. Several observations can be made based on the results presented in Figure 6:

1. The dissolution process is initially diffusion-dominated for all cases. The departure from diffusive mixing depends on the magnitude of the permeability variation field;
2. Convective mixing can increase rate of dissolution significantly; and,
3. Formation heterogeneities play a significant role in enhancing the rate of dissolution.

From the dissolution curves in Figure 6 it is clear that, for heterogeneous porous media (Cases 2 to 5), the time for the onset of instability is much smaller than that predicted by the theoretical criterion for onset of instability in homogenous formations. The role of heterogeneity on generation of instability and convective mixing is not well understood and requires more attention.

Case Studies for Two Alberta Basin Aquifers

A moderate efficiency coal-fired power plant generates approximately 1 kg of CO_2 per each kWh of generated electrical energy. A number of coal-fired power plants with total capacity of more than 4,000 MW are located near Lake Wabamun in central Alberta, Canada[40]. The capacity of the aquifers in the region to sequester CO_2 needs investigation. The Nisku aquifer is regionally confined by the thick Exshaw aquitard. Law and Bachu[40] used a multicomponent, multiphase reservoir simulator to simulate the geological CO_2 sequestration. In their work, a two-dimensional radial grid was used to simulate CO_2 injection in a single well. Pure CO_2 was injected for 30 years and the injection pressure was allowed to increase to 90% of the rock fracturing pressure. They found that

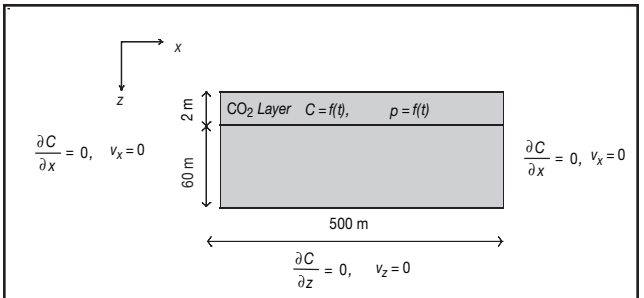

FIGURE 7: Model geometry and boundary conditions for the Nisku aquifer.

the reservoir porosity has a small effect on the amount of CO_2 injected, reservoir thickness has a moderate effect, and the absolute permeability has the most important effect. They studied the interactions between the injected CO_2 and the brine over a period of 30 years. Their simulation results showed that within this period most of the CO_2 would migrate to the top.

In this study, simulations are performed using data from Reference 40 to investigate the role of convection and diffusion on the long-term dissolution of the CO_2 after it has migrated to the top, and to provide a rough estimate for the time of dissolution.

First, a vertical cross section of 500 m wide of the Nisku aquifer was selected for numerical simulation. The model geometry and boundary conditions are depicted in Figure 7 and the data are given in Table 4. It is assumed that by the time injection has stopped, the injected CO_2 has formed a CO_2 cap of thickness 2 m beneath the sealing formation. The cap pressure is allowed to vary with time as CO_2 diffuses into the underlying brine. Brine viscosity is assumed constant (0.5 mPa•s) and, similar to the mechanistic study, 1% increase of density is assumed due to maximum dissolution. Using Equation (7) and the input data for this problem, the Rayleigh number is approximately 429, implying that instabilities should arise.

Simulations were performed using different numbers of grid blocks to examine the role of numerical instabilities. In order to ensure that the numerical perturbations are not the cause of convective mixing, the appropriate Courant and grid Peclet number criteria were honoured and a permeability field with a small random variation of 0.1% was imposed using GSLIB software[39]. It is expected that the permeability variation of the natural setting is more than 0.1%, leading to a faster onset of instabilities. The ratio of vertical to horizontal permeability was taken at 0.30. The results, presented in Figures 8 and 9, belong to a case where the domain was discretised to 1,000 by 100 grid blocks in horizontal and vertical directions, respectively. The simulation was started with a time step of 0.32 years, which was subsequently controlled based on the model convergence. The maximum time step used in the simulation was one year. Figure 8 shows the evolution of density-driven instability at different times for the Nisku aquifer.

Figure 9 shows the dissolution of carbon dioxide in the aquifer vs. time with and without convective mixing. The period of diffusion dominated mixing is about 160 years. Complete dissolution of CO_2 in the aquifer by pure diffusion will take thousands of years, whereas this time is much smaller in the presence of convective mixing. Results given in Figure 9 suggest that in the presence of convective mixing, the aquifer will dissolve more than 60% of its ultimate dissolution capacity in 800 years.

Because of the CO_2 dissolution in the aquifer, the top boundary pressure varies with time. Figure 10 shows pressure variations as function of time for the Nisku aquifer. Pressure at the boundary drops slightly with time during the diffusion period and there is a

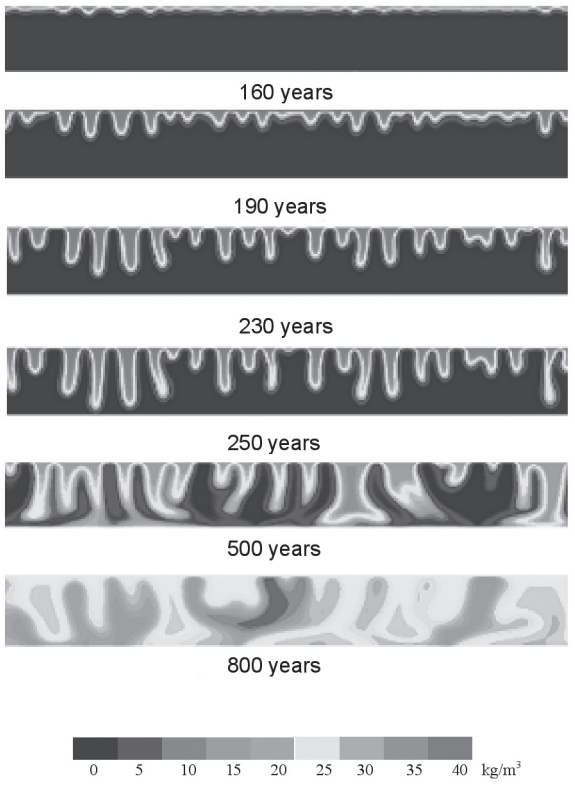

FIGURE 8: Evolution of convection mixing in the Nisku aquifer at different times while the top boundary pressure varies with time. Plates show the CO_2 concentration distribution for a case discretised into a 1,000 × 100 grid block system.

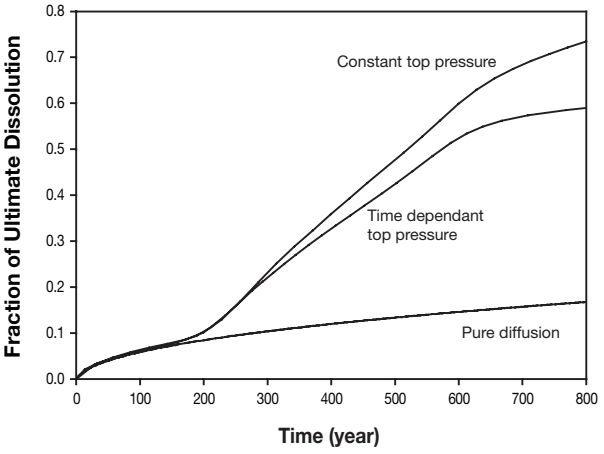

FIGURE 9: Fraction of ultimate dissolution for the Nisku aquifer for different cases.

sharp pressure drop due to the action of convective mixing, which dissolves a large volume of CO_2 into the aquifer.

The above simulation studies consider closed boundaries for the aquifer, after the CO_2 cap is established. In actual cases, as CO_2 dissolves in the aquifer and pressure drops, more water flows inward and partially maintains the pressure. At higher pressures, the aquifer can dissolve more of the CO_2. It is therefore believed that the above simulations, with closed boundaries, give an upper bound for the time of CO_2 dissolution. To obtain a lower bound for the time of dissolution, a case was run where the CO_2 cap pressure was kept constant. The upper curve in Figure 9 shows a higher fraction of ultimate dissolution for this case and indicates that more of the CO_2 is dissolved if there is a pressure support mechanism in

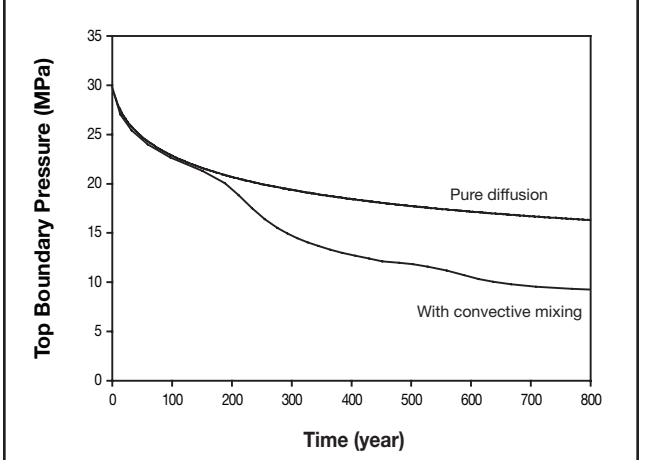

FIGURE 10: Variation of CO_2 equilibrium pressure at the top boundary, the Nisku aquifer case.

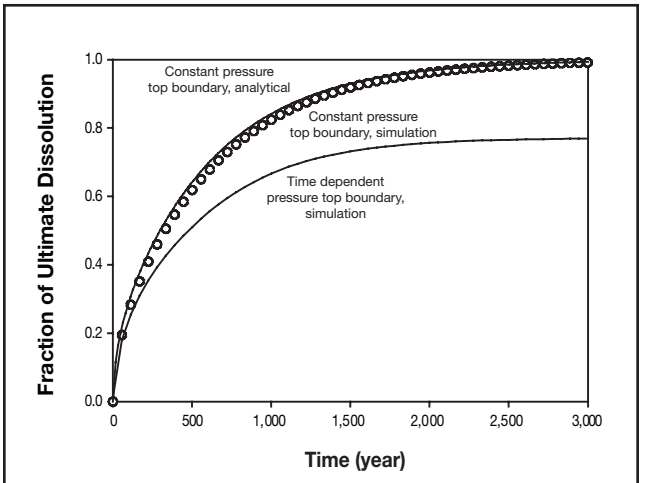

FIGURE 11: Fraction of ultimate dissolution for Glauconitic sandstone aquifer using 1,000 × 20 grid block system.

the aquifer. Results reveal that the convective mixing greatly accelerates the dissolution process and the remaining CO_2 in the cap is significantly reduced in the presence of convective mixing and a pressure support mechanism.

Next, CO_2 sequestration in the Glauconitic sandstone aquifer in the Alberta basin was studied. The related data are given in Table 4[40]. It was assumed that after injection has ceased, the injected CO_2 formed a cap of thickness 1.0 m beneath the sealing formation. Substituting the data for this problem into Equation (7), the calculated Rayleigh number is 14. This is less than the critical Rayleigh number necessary for formation of convective cells, hence it is expected that convective mixing will not occur. Simulation results for a limited size aquifer with varying CO_2 pressure are shown in Figure 11 and indicate that no convective mixing occurs in about 3,000 years of simulation.

For a case of constant CO_2 cap pressure, it is possible to develop an analytical solution for the diffusive mixing process. The governing equation and its initial and boundary conditions are given by:

$$\frac{\partial^2 C}{\partial z^2} = \frac{1}{D}\frac{\partial C}{\partial t} \qquad C(z,0) = 0 \qquad C(0,t) = 1$$

and

$$\frac{\partial C}{\partial z}(H,t) = 0 \qquad \text{..... (9)}$$

The solution to the above problem is obtained by using the separation of variables method and given by:

$$C(z,t) = 1 - \frac{4}{\pi}\sum_{n=0}^{\infty}\left(\frac{1}{2n+1}\right)\sin\left[\left(\frac{2n+1}{2H}\pi\right)z\right] \exp\left[-\left(\frac{2n+1}{2H}\pi\right)^2 Dt\right]. \quad \text{..... (10)}$$

The amount of CO_2 dissolved in the aquifer can be obtained by taking a depth average of the concentration profile, as expressed in the following:

$$\overline{C}(t) = 1 - \frac{8}{\pi^2}\sum_{n=0}^{\infty}\left(\frac{1}{2n+1}\right)^2 \exp\left[-\left(\frac{2n+1}{2H}\pi\right)^2 Dt\right] \quad \text{.....(11)}$$

A numerical simulation was performed using the Glauconitic aquifer data. The domain was discretised to 1,000 × 20 grid block system and a constant time step of 1.5 years was used in the simulation. Figure 11 shows a comparison between the analytical and numerical simulations for the constant CO_2-cap pressure. Figure 11 shows that the case of constant CO_2-cap pressure leads to 23% increase in fraction of ultimate dissolution as compared to the time-dependent top pressure. Results for this Glauconitic sandstone aquifer case show that the dominant dissolution mechanism is pure diffusion.

Conclusion

A numerical model was developed to study the dissolution of CO_2 in aquifers. Results indicate that accurate numerical solution of density-driven flow requires satisfying the grid-Peclet and Courant number conditions presented in the paper. This requires very small grid blocks when the diffusion coefficient is small. It is expected that the accurate modelling of CO_2 fingers with their small widths could pose a numerical challenge for field scale simulations. The model presented in this work was validated against a benchmark problem of density-driven flow in porous media. Results show a good agreement between the model and the reference solution.

Geological CO_2 sequestration was then simulated in three different aquifer cases with different physical properties. The results show that for two cases, including the Nisku aquifer, convective mixing occurs and significantly improves the dissolution rate of CO_2. It was confirmed that the onset of free convection predicted by the model agrees well with the theoretical time to the onset of free convection.

Based on the results presented in this paper, the following conclusions about the dissolution of CO_2 into the underlying brine are drawn:

- The diffusion of CO_2 into underlying brine increases its density. The presence of the higher density fluid above the low density fluid can lead to the formation of convective flow fields, which increase the dissolution rate significantly;
- For cases that lead to convective mixing, two timescales are important. The first is the onset of instability, and the second is the timescale for convection mixing to distribute the CO_2 throughout the aquifer;
- The time to the onset of instability, if it occurs, depends on the Rayleigh number and the heterogeneity of the formation;
- The theoretical onset of instability available in the literature is for homogeneous formations and is not applicable for heterogeneous formations. The role of heterogeneity on growth and decay of instability fingers is of practical importance and requires more investigation;
- For the Nisku aquifer case, convective mixing greatly accelerated dissolution of CO_2. For this case, more than 65% of the original CO_2 was dissolved in 800 years; and,
- In the case of the Glauconitic sandstone aquifer case, the aquifer physical properties were such that the convective mixing could not occur. In this case, the dominant dissolution mechanism was diffusion.

Acknowledgements

Financial support for this work was provided by the National Science and Engineering Research Council of Canada (NSERC). Computer facilities were provided through a CFI grant. This support is gratefully acknowledged. The first author wishes to acknowledge the financial support of the National Iranian Oil Company (NIOC) during the course of this study.

NOMENCLATURE

C = concentration, kg of solute/m^3 solution
C_i = initial CO_2 concentration, kg of solute/m^3 solution
C^* = equilibrium concentration, kg of solute/m^3 solution
C_R = Courant number, dimensionless
$\overline{C}$ = average concentration, kg of solute/m^3 solution
c = ultimate dissolution, kg
D = molecular diffusion coefficient, m^2/s
g = acceleration of gravity, m/s^2
H = formation thickness, m
h = depth of grid block, m
k = permeability, m^2
n = summation index
Pe = Peclet number, dimensionless
p = pressure, Pa.
Ra = Rayleigh number, dimensionless
t = time, s
t_c = critical time, s
v^c = Darcy velocity, m/s
V_p = aquifer pore volume, m^3
z = depth from aquifer top, m
β_ρ = coefficient of density increase due to dissolution, m^3 of solution/kg of solute
Δl = grid block size, m
ρ = fluid density, kg/m^3
$\Delta\rho$ = fluid density increase, kg/m^3
ϕ = porosity, dimensionless
μ = viscosity, Pa•s
ρ_0 = original fluid density, kg/m^3

REFERENCES

1. TANAKA, T.S. and HAKUTA, H.H., Possible Contribution of Carbon Dioxide Flooding to Global Environmental Issues; *Energy Conversion and Management, Vol. 33, Nos. 5 – 8, pp. 587-593, May – August 1992.*
2. SHAW, J.C. and BACHU, S., Screening, Evaluation, and Ranking of Oil Reservoirs Suitable for CO_2-Flood EOR and Carbon Dioxide Sequestration; *Journal of Canadian Petroleum Technology, Vol. 41, No. 9, pp. 51-61, 2002.*
3. BACHU, S. and GUNTER, W.D., Overview of Acid-Gas Injection Operations in Western Canada; *proceedings of the 7th International Conference on Greenhouse Gas Control Technologies*, *Vol. 1: (E.S. Rubin, D.W. Keith and C.F. Gilboy, ed.), IEA Greenhouse Gas Programme, Cheltenham, UK, 2005 (in press).*
4. BACHU, S. and CARROLL J.J., In Situ Phase and Thermodynamic Properties of Resident Brine and Acid Gases (CO_2 and H_2S) Injected in Geological Formations in Western Canada; *proceedings of 7th International Conference on Greenhouse Gas Control Technologies, Vol. 1: (E.S. Rubin, D.W. Keith and C.F. Gilboy, ed.), IEA Greenhouse Gas Programme, Cheltenham, UK, 2005 (in press).*
5. LINDEBERG, E.G.B. and WESSEL-BERG, D., Vertical Convection in an Aquifer Column Under a Gas Cap of CO_2; *Energy Conversion and Management, Vol. 38 Supplement, pp. 229-234, 1996.*

6. GUNTER, W.E., PERKINS, E.H., and WIWCHAR, B., Aquifer Disposal of CO_2-Rich Greenhouse Gases: Extension of the Time Scale of Experiment for CO_2-Sequestering Reactions by Geochemical Modelling; *Mineralogy and Petrology, Vol. 59, pp. 121-140, 1997.*
7. AZIZ, K. and SETTARI, A., Petroleum Reservoir Simulation; *Elsevier Applied Scientific Publisher, 1979.*
8. CHANDRASEKHAR, S., Hydrodynamic and Hydromagnatic Stability; *Oxford at the Clarendon Press, 1961.*
9. SIMMONS, C.T., FENSTEMAKER, T.R., and SHARP, J.M., Variable-Density Groundwater Flow and Solute Transport in Heterogeneous Porous Media: Approaches, Resolutions and Future Challenges; *Journal of Contaminant Hydrology, Vol. 52, Issues 1 – 4, pp. 245-275, November 2001.*
10. KOLDITZ, O., RATKE, R., DIERSCH, H.-J., and ZIELKE, W., Coupled Groundwater Flow and Transport: 1. Verification of Variable Density Flow and Transport Models; *Advances in Water Resources, Vol. 21, Issue 1, pp. 27-46, February 1998.*
11. ACKERER, PH., YOUNES, A., and MOSE, R., Modelling Variable Density Flow and Solute Transport in Porous Medium: 1. Numerical Model and Verification; *Transport in Porous Media, Vol. 35, No. 3, pp. 345-373, June 1999.*
12. YOUNES, A., ACKERER, P.H., and MOSE, R., Modelling Variable Density Flow and Solute Transport in Porous Medium: 2. Re-Evaluation of the Salt Dome Flow Problem; *Transport in Porous Media, Vol. 35, No. 3, pp. 375-394, June 1999.*
13. YOUNES, A., On Modelling the Multidimensional Coupled Fluid Flow and Heat or Mass Transfer in Porous Media; *International Journal of Heat and Mass Transfer, Vol. 46, pp. 367-379, 2003.*
14. IBARAKI, M., A Robust and Efficient Numerical Model for Analyses of Density-Dependent Flow in Porous Media; *Journal of Contaminant Hydrology, Vol. 34, Issue 3-31, pp. 235-246, October 1998.*
15. User's Guide to SEAWAT: A Computer Program for Simulation of Three-Dimensional Variable Density Ground-Water Flow; *U.S. Geological Survey,* 2002.
16. PICARD, C.E., Journale de Math; *Vol. 4, No. 6, pp. 145-210, 1890.*
17. SEGOL, G., Classical Groundwater Simulations, Proving and Improving Numerical Models; *PTR Prentice Hall, 1994.*
18. BURNETT, R.D. and FRIND, E.O., Simulation of Contaminant Transport in Three Dimensions, 1, The Alternate Direction Galerkin Technique; *Water Resources Research, Vol. 23, No. 4, pp. 689-90, 1987.*
19. BURNETT, R.D. and FRIND, E.O., Simulation of Contaminant Transport in Three Dimensions, 1, Dimensionality Effects; *Water Resources Research, Vol. 23, No. 4, pp. 695-705, 1987.*
20. ELIASSI, M. and GLASS, R.J., On the Continuum-Scale Modelling of Gravity Driven Fingers in Unsaturated Porous Media: The Inadequacy of the Richards Equation With Standard Monotonic Constitutive Relations and Hysterestic Equations of State; *Water Resources Research, Vol. 37, No. 8,* pp. 2019-2035, August 2001.
21. ELDER, J.W., Steady Free Convection in a Porous Medium Heated From Below*; Journal of Fluid Mechanics, Vol. 27, pp. 29-50, 1967.*
22. ELDER, J.W, Transient Convection in a Porous Medium; *Journal of Fluid Mechanics, Vol. 27, pp. 609–623, 1967.*
23. VOSS, C.I. and SOUZA, W.R., Variable Density Flow and Solute Transport Simulations of Regional Aquifers Containing a Narrow Freshwater-Saltwater Transition Zone; *Water Resources Research, Vol. 23, pp. 1851-1866, 1987.*
24. SIMPSON, M.J. and CLEMENT, T.P., Theoretical Analysis of the Worthiness of Henry and Elder Problems as Benchmarks of Density-Dependent Groundwater Flow Models; *Advances in Water Resources, Vol. 26, Issue 1, pp. 17-31, January 2003.*
25. TENG, H., YAMASAKI, A., CHUN, M.K., and LEE, H., Solubility of Liquid CO_2 in Water at Temperatures From 278 K to 293 K and Pressures From 6.44 MPa to 29.49 MPa and Densities of the Corresponding Aqueous Solutions; *Journal of Chemical Thermodynamics, Vol. 29, pp. 1301-1310, 1997.*
26. GARCIA, J.E., Density of Aqueous Solutions of CO_2; *Report LBNL-49023, Lawrence Berkeley National Laboratory, A, p. 8, 2001.*
27. ENNIS-KING, J. and PATERSON, L., Role of Convective Mixing in The Long-Term Storage of Carbon Dioxide in Deep Saline Formations; *SPE paper 84344, 2003.*
28. ENNIS-KING, J. and PATERSON, L., Rate of Dissolution due to Convective Mixing in the Underground Storage of Carbon Dioxide; *Proceedings of the 6th International Conference on Greenhouse Gas Control Technologies, 2002.*
29. HASSANZADEH, H., POOLADI-DARVISH, M., KEITH, W.D., and LEONENKO, Y., Predicting Thermodynamic and Transport Properties of a CO_2-Water Mixture for Geological Storage; *(submitted to Petroleum Society).*
30. WIEBE, R. and GADDY, VL., The Solubility in Water of Carbon Dioxide at 50, 75, and 100° C at Pressure to 70 Atmospheres; *Journal of the American Chemical Society, Vol. 61, pp. 315, 1940.*
31. HALL, K.R. and YARBOROUGH, L., A New Equation-of-State for Z-Factor Calculation; *Oil and Gas Journal, pp. 82-92, June 1969.*
32. BACHU, S. and ADAMS, J.J., Sequestration of CO_2 in Geological Media in Response to Climate Change: Capacity of Deep Saline Aquifers to Sequester CO_2 in Solution; *Energy Conversion and Management, Vol. 44, Issue 20, pp. 3151-3175, December 2003.*
33. HORTON, C.W. and ROGERS, JR., F.T., Convection Currents in a Porous Medium; *Journal of Applied Physics, Vol. 16, pp. 367-370, 1945.*
34. WOODING, R.A., Steady State Free Thermal Convection of Liquid in a Saturated Porous Medium; *Journal of Fluid Mechanics, Vol. 2, pp. 273-285, 1956.*
35. KATTO, Y. and MASUOKA, T., Criterion for the Onset of Convective Flow in a Fluid in a Porous Medium; *International Journal of Heat and Mass Transfer, Vol. 10, pp. 297-309, 1967.*
36. TAN, K.K., SAM, T., and JAMALUDIN, H., The Onset of Transient Convection in Bottom Heated Porous Media; *International Journal of Heat and Mass Transfer, Vol. 46, Issue 15, pp. 2857-2873, July 2003.*
37. TAN, K.K. and THORPE, R.B., The Onset of Convection Driven By Buoyancy Effects Caused by Various Modes of Transient Heat Conduction: Part I. Transient Rayleigh Numbers; *Chemical Engineering Science, Vol. 54, Issue 2, pp. 225-233, March 1999.*
38. TAN, K.K. and THORPE, R.B., The Onset of Convection Driven by Buoyancy Effects Caused by Various Modes of Transient Heat Conduction: Part II. The Sizes Of Plumes; *Chemical Engineering Science, Vol. 54, Issue 2, pp. 239-244, January 1999.*
39. DEUTSCH, C.V. and JOURNEL, A.G., Gslib: Geostatistical Software Library and User's Guide; *Oxford University Press, 1997.*
40. LAW, D.H.-S. and BACHU, S., Hydrogeological and Numerical Analysis of CO_2 Disposal in Deep Aquifers in the Alberta Sedimentary Basin; *Energy Conversion and Management, Vol. 37, Issues 6 – 8, pp. 1167-1174, 1996.*

Provenance—Original Petroleum Society manuscript, **Modelling of Convective Mixing in CO_2 Storage** (2004-151), first presented at the 5th Canadian International Petroleum Conference (the 55th Annual Technical Meeting of the Petroleum Society), June 8 - 10, 2004, in Calgary, Alberta. Abstract submitted for review December 8, 2003; editorial comments sent to the author(s) May 11, 2005; revised manuscript received May 27, 2005; paper approved for pre-press August 8, 2005; final approval September 23, 2005.

Authors' Biographies

Hassan Hassanzadeh is currently a Ph.D. student at the University of Calgary Department of Chemical and Petroleum Engineering. Hassan received a B.Sc. in petroleum engineering from the Petroleum University of Technology in 1994 and an M.Sc. in chemical engineering from Tehran University in 1997, both in Iran. Hassan worked as a production engineer with the National Iranian Oil Company (NIOC) for seven years. His research interests are analytical and numerical modelling of transport phenomena in porous media with applications to geological gas storage, natural convection, and upscaling of fluid flow parameters for fractured reservoirs simulation. He is a member of the Petroleum Society and SPE.

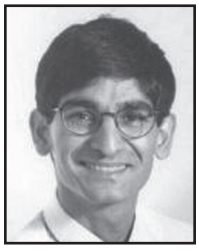

Mehran Pooladi-Darvish is an associate professor of petroleum engineering at the University of Calgary where he teaches reservoir engineering and well testing courses. His current research activities are on experimental and modelling studies of cold production of heavy oil, upscaling methods in naturally fractured reservoirs, and gas production from hydrate reservoirs. He is the winner of the "Best Paper Published in JCPT 2000 Award" and has been featured as a distinguished author in the Journal of Petroleum Technology (June 2004). Mehran has previously worked at the Reservoir Engineering Research Institute, Palo Alto, CA, and in Ahwaz, Iran. He has appeared as an expert witness at the Alberta Energy and Utility Board hearings on gas over bitumen. Mehran received a B.Sc. in chemical engineering (1989) and a M.Sc. in chemical and petroleum engineering (1992) from Iran. He graduated with a Ph.D. in petroleum engineering from the University of Alberta (1995).

David Keith is currently the Canada Research Chair in Energy and the Environment and a professor in the Department of Chemical and Petroleum Engineering and the Department of Economics at the University of Calgary. Professor Keith works near the interface between climate science, energy technology, and public policy. Much of his policy work is focused on the capture and storage of CO_2, including services as chair of a crosscutting group for the IPCC special report on CO_2 storage and as a member of U.S. National Academy committees. Keith's broader climate and energy related research addresses the economics and climatic impacts of large-scale wind power, the use of hydrogen as a transportation fuel, and the technology and implications of geoengineering. Keith's has addressed technical audiences with articles in *Science* and *Nature*. He has consulted for national governments, industry and environmental groups, and has reached the public through U.S. and Canadian radio and television. Keith is trained as a physicist. As a graduate student at MIT, he built the first interferometer for atoms work which was the hottest topic in physics according to ISI's Citation Index algorithms. As an atmospheric scientist, he worked at NCAR and Harvard, where he served as lead scientist for a new Fourier-transform spectrometer with high radiometric accuracy that flies on the NASA ER-2 high-altitude aircraft. Keith returned to Canada in 2004, taking a position at the University of Calgary where he is working to build a high-quality research group working on energy and environmental systems.